Coordinated allele-specific histone acetylation at the differentially methylated regions of imprinted genes

Purnima Singh[1], Janice Cho[1,2,3], Shirley Y. Tsai[1], Guillermo E. Rivas[4], Garrett P. Larson[4] and Piroska E. Szabó[1,*]

[1]Department of Molecular and Cellular Biology, [2]Eugene and Ruth Roberts Summer Student Academy, City of Hope National Medical Center, Duarte, CA 91010, [3]Pitzer College, Claremont, CA 91711 and [4]Department of Molecular Medicine, City of Hope National Medical Center, Duarte, CA 91010, USA

ABSTRACT

Genomic imprinting is an epigenetic inheritance system characterized by parental allele-specific gene expression. Allele-specific DNA methylation and chromatin composition are two epigenetic modification systems that control imprinted gene expression. To get a general assessment of histone lysine acetylation at imprinted genes we measured allele-specific acetylation of a wide range of lysine residues, H3K4, H3K18, H3K27, H3K36, H3K79, H3K64, H4K5, H4K8, H4K12, H2AK5, H2BK12, H2BK16 and H2BK46 at 11 differentially methylated regions (DMRs) in reciprocal mouse crosses using multiplex chromatin immuno precipitation SNuPE assays. Histone acetylation marks generally distinguished the methylation-free alleles from methylated alleles at DMRs in mouse embryo fibroblasts and embryos. Acetylated lysines that are typically found at transcription start sites exhibited stronger allelic bias than acetylated histone residues in general. Maternally methylated DMRs, that usually overlap with promoters exhibited higher levels of acetylation and a 10% stronger allele-specific bias than paternally methylated DMRs that reside in intergenic regions. Along the *H19/Igf2* imprinted domain, allele-specific acetylation at each lysine residue depended on functional CTCF binding sites in the imprinting control region. Our results suggest that many different histone acetyltransferase and histone deacetylase enzymes must act in concert in setting up and maintaining reciprocal parental allelic histone acetylation at DMRs.

INTRODUCTION

Epigenetics involves changes in phenotypes and gene expression due to factors other than DNA sequence itself. DNA methylation and the spatial organization of DNA at several levels are major players of the epigenetic regulation. The first level of DNA spatial organization occurs at the level of nucleosomes. The nucleosome core particle consists of 147 bp of DNA wrapped around an octamer of highly conserved core histones with two copies each of H2A, H2B, H3 and H4. The tails and globular domains of the core histones can be covalently modified at specific amino acids and the combinatorial readout of the histone covalent modifications provides clues to gene regulation to activate, poise or repress transcription. Histone covalent modifications undergo dynamic global and local changes during development, cell division and cell activation. Reversible acetylation at the internal histone lysine positions has traditionally been considered to correspond to the transcriptionally active state (1–4). Histone acetyltransferases (HATs) and histone deacetylases (HDACs) are responsible for setting up steady-state levels of histone acetylation levels. Both HATs and HDACs are present in the active/poised 0.15 M NaCl-soluble chromatin fraction (5,6). Genome-wide mapping revealed that these opposite activities are indeed co-localized at active loci (7). Gene regulation via histone acetylation can be very robust because of the large number of acetylatable lysine residues. It can also present opportunities for fine tuning, because each core histone has more than one lysines and each can exist in either acetylated or unmodified or methylated form. Mutually exclusive acetylation and methylation of lysines H2BK5, H3K4, H3K9, H3K27 and H3K36 were detected at specific genomic loci (7), and this likely holds true for other lysines.

There are some indications to suggest that acetylation at different lysine residues in the four core histones carries functionally distinct clues. HATs and HDACs exhibit site specificities for certain lysine residues. Acetylation sites are extremely conserved in H3 and H4 but less conserved in H2A and H2B. Acetylation of the different lysine residues is not uniform, some (H2AK9ac, H2BK5ac, H3K9ac, H3K18ac, H3K27ac, H3K36ac and H4K91ac) show a robust peak at the transcription start site (TSS) of active and poised genes, others (H2BK12ac, H2BK20ac, H2BK120ac, H3K4ac, H4K5ac, H4K8ac, H4K12ac and H4K16ac) exhibit enrichment at the TSS and along gene bodies (8). Several lysine acetylation sites (H2BK5, H2BK12, H2BK20, H2BK120, H3K4, H3K9, H3K18, H3K27, H3K36, H4K5, H4K8 and H4K91) belong to the 'common modification module' found at active/poised promoters, consisting of 17 out of 39 tested histone modifications (8). Lysine acetylation, however, is not found in gene deserts and at constitutive heterochromatin regions except for H2AK5ac and H3K14ac at subtelomeres (9). Utilization of the lysine positions is not random: newly synthesized histones emerge with acetylated lysines at preferred positions and other lysine residues follow in a sequential manner (10–12). Acetylation or lack of acetylation of each lysine residue may have different roles in the combinatorial readout. Mutagenesis of individual lysine residues in the globular domain had more serious consequence than that of lysines in the histone tails causing severe defects in silent chromatin formation and DNA repair in yeast (13–15).

Imprinted genes exhibit parent-of-origin specific monoallelic expression. In somatic cells, the paternally and maternally inherited alleles of imprinted genes exist in opposite epigenetic states, characterized by allele-specific DNA methylation and also histone covalent modifications. Gamete-specific DNA methylation marks are established at germ line differentially methylated regions (DMRs) (16,17) in the male and female germ lines by the *de novo* DNA methyltransferases Dnmt3a and Dnmt3b together with Dnmt3L (18–20) and are maintained during somatic cell division in the paternal and maternal alleles, respectively. DNA methylation at DMRs is essential for the allele-specific expression of most imprinted genes (21). Imprinting control regions (ICRs) are DMRs with the capacity to control the monoallelic expression of the associated genes in the respective domains (22–29). Histone acetylation distinguishes the unmethylated alleles of imprinted genes and DMRs in the soma (30–53) and marks the maternally methylated DMRs in postnatal male germ cells (31). Allele-specific histone acetylation at least at the maternally methylated DMRs depends on gametic DNA methylation differences (37).

In the *H19/Igf2* imprinted region, the ICR DMR regulates monoallelic expression of the oppositely imprinted *H19* and *Igf2* genes (25,54,55). The CCCTC-binding factor (CTCF) insulator binds in the unmethylated maternal ICR allele and blocks communication between the *Igf2* promoters and the shared downstream enhancers. CTCF binding is inhibited in the paternal ICR allele by DNA methylation, allowing *Igf2* promoter access to the enhancers (56–60). ICR CTCF-site mutations in the maternal allele result in biallelic *Igf2* expression and *H19* repression (36,61–63). CTCF is the single most important factor responsible for organizing the allele-specific chromatin along the *H19/Igf2* imprinted domain (36). This involves recruiting H3K9 acetylation to the maternal allele at the *H19* locus/ICR region and excluding H3K9ac from the maternal allele at the *Igf2* locus.

Allele-specific histone acetylation has been assessed at DMRs at a number of lysine residues (H3K9ac/K14ac, H3K9ac, H4K14ac, H3K9/K18ac, H3K27ac, H4K5, H4K8, H4K16 and H4K12), but only a few of these were tested at once at a small set of imprinted genes. A general assessment of histone acetylation at DMRs is still lacking. It is not known whether histone acetylation distinguishes parental alleles of each DMR or whether the strength of the allele-specific bias is different between the four core histones. It is not known if histone acetylation at maternally and paternally methylated DMRs exhibits any difference in marking the hypomethylated allele. We hypothesized that maternally methylated DMRs may be more distinguished by acetylated histones than paternally methylated DMRs, because the former are associated with promoters, whereas the latter reside in intergenic regions (64). We wondered if the 'common modification module' (8) residues behave differently from others with respect to marking the parental alleles of DMRs. To address these questions, we mapped the parental allele-specific histone acetylation of thirteen lysine residues at three paternally- and eight maternally methylated mouse DMRs. Additionally, we asked whether the allele-specific acetylation at each lysine residue responds to CTCF site mutations along the *H19/Igf2* imprinted domain.

MATERIALS AND METHODS

Chromatin immunoprecipitation in MEF

MEFs were derived from 13.5 dpc embryos. Chromatin was prepared from 129 X CS, CS X 129, CTCFm X CS, 129 X JF1 and JF1 X 129 primary MEFs as described earlier (36). The chromatin was crosslinked for 2 m [N-chromatin immunoprecipitation (ChIP)] or 10 m (X-ChIP) with formaldehyde and sonicated in lysis buffer. An aliquot of the chromatin was reverse-crosslinked, quantified by OD and the efficiency of sonication was assessed on agarose gel. Sonicated chromatin was then diluted to 0.4 mg/ml concentration and snap-frozen in small aliquots. One aliquot was thawed on the day of ChIP. The ChIP was performed as described earlier (36) with minor modifications. Pre-blocked A/G beads from Santa Cruz (Cat#sc-2003) were used for capturing the precipitated chromatin. The antibodies used in the ChIP assays are listed in Supplementary Table S1. N-ChIP conditions were used for the H3K18ac antibody and X-ChIP conditions were used for all of the other antibodies.

Cross-linking chromatin from 13.5 dpc embryos

Chromatin was prepared from the body, head and placenta of 13.5 dpc embryos resulting from a JF1

mother X 129 father cross. The embryo part excluded the liver and the gonads. The body, head and placenta were suspended in 1 ml ice-cold phosphate buffered saline (PBS) without Calcium and Magnesium and dissociated by gentle application of eppendorf pestle. An aliquot was saved for RNA analysis, which was performed as we reported earlier (65). Thirty-seven percent formaldehyde was directly added to the cell suspension at a final concentration of 1% to crosslink chromatin and it was gently rotated at room temperature for 10 m. The crosslinking was stopped by adding 104 μl of 1.25 M glycine followed by gentle rotation at RT for 10 m. The cells were collected by centrifugation at 250 g for 5 m, washed twice with ice cold PBS and resuspended in ChIP Lysis Buffer (1% SDS, 10 mM EDTA and 50 mM Tris-HCl, pH 8.1) containing protease inhibitors. Four micrograms of crosslinked sonicated chromatin was used per ChIP.

Real-time PCR

Real-time PCR was performed to measure the region-specific overall ChIP enrichment levels at the *H19-Igf2* domain (36) and at eleven DMRs (65) as described. Three microliter aliquots of the ChIP elution DNA were amplified with region-specific primers. A dilution series of genomic DNA was used for quantifying copy numbers from ChIP and input samples. PCR primers for the 11 DMRs and control regions were described earlier (65) and are also provided in Supplementary Table S2.

Analysis of allele-specific histone enrichment

To measure allele-specific chromatin differences we used the matrix-assisted laser desorption/ionization time-of-flight mass spectrometry (MALDI-TOF) allelotyping analysis method on the Sequenom platform as described earlier (65). This method uses mass spectrometry quantification of the extended SNuPE primers based on the differences in molecular mass between alleles. A 16-plex assay was used for 11 DMRs and a 7-plex assay was used for the *H19/Igf2* imprinted domain. The percent expression of each allele in the total expression was calculated at each given SNP. Primers for the 11 DMRs and control regions were described earlier (65) and are provided in Supplementary Table S2.

RESULTS

Assessment of the specificity of the antibodies

To gain an insight into how general allele-specific histone acetylation is at DMRs, we used a comparative and comprehensive chromatin analysis at a large set of germ line DMRs with 13 antibodies against different acetylated histone residues. The H3K36ac, H4K79ac, H4K5ac, H4K12ac antibodies and control H4K16ac antibodies recognized the corresponding acetylated peptides in immuno-dot blot assays with high specificity (Supplementary Figure S1). Data obtained with these antibodies can be interpreted with high confidence (spec>> in Table 1). The data with the remaining

antibodies needs to be interpreted with caution. The H4K8ac, H2BK16ac and control H3K9ac antibodies recognized the corresponding acetylated peptide with high specificity but the unmodified peptide was not tested. The H3K27ac, H3K64ac and H2BK46ac antibodies recognized the corresponding acetylated peptide but cross-reacted with the unmodified peptide of the same lysine residue. These six antibodies are classified in the less specific category (spec> in Table 1). The H3K18ac antibody cross-reacted with the H2BK16ac peptide. The specificity of H2AK5ac, H3K4ac and H2BK16ac antibodies were not tested because these peptides were not available.

Measuring allele-specific histone acetylation at eleven germ line DMRs

We tested three paternally and eight maternally methylated germ line DMRs for allele-specific histone acetylation using our recently developed 16-plex ChIP-SNuPE assays (65). Four of the DMRs were represented in the assay with two or three alternative SNPs along their sequences. The ChIP-SNuPE assays determine the ratio of maternal or paternal allele in the total immunoprecipitation by measuring the incorporation of dideoxy nucleotides at sites of single nucleotide polymorphisms between 129 and JF1 mouse genomic DNA.

Histone acetylation at eight maternally and three paternally methylated DMRs in MEFs

We precipitated chromatin from primary MEFs of 129 X JF1 and reciprocal JF1 X 129 mouse crosses using the antibodies for the specific acetylated lysine residues H3K4, H3K18, H3K27, H3K36, H3K79, H3K64, H4K5, H4K8, H4K12, H2AK5, H2BK12, H2BK16 and H2BK46. Real-time PCR quantitation of the ChIP DNA showed that these antibodies very strongly precipitated an euchromatin control region at the *c-myc* promoter but weakly precipitated the constitutive heterochromatin control regions, IAP and major satellites, as expected, and also the *Oct4* promoter, which is silent in MEFs (Supplementary Table S3). At the DMRs most antibodies precipitated the chromatin at higher level than the non-specific IgG, with some exceptions (white cells in Supplementary Tables S4 and S5). The DMRs were generally less acetylated than the *c-myc* promoter but more acetylated than the heterochromatin control regions. This was expected, because only one allele of each DMR is in the euchromatin state. Interestingly, the maternally methylated DMRs (Supplementary Table S5) exhibited higher level of overall acetylation than the paternally methylated DMRs (Supplementary Table S4).

We then subjected the precipitated chromatin preparations to allele-specific multiplex DMR ChIP-SNuPE assays. We have previously reported that H3K9ac exhibited a very strong bias toward the paternal allele at each maternally methylated DMR and maternal allele-specific bias at each paternally methylated DMR (65). Each of the DMRs (16) with maternal allele-specific CpG methylation (*Peg1-Mest*, *Zac1*, *Gnas1A*, *Peg3*, *Snrpn*, KvDMR1, *Igf2r* DMR2 and *U2af1*) exhibited a strong

Table 1. Summary of allele-specific acetylation at DMRs in MEFs

Histone	Antibody	Domain	CMM	Localization	Specificity	All data		Filtered data	
						MAT DMR PAT allele	PAT DMR MAT allele	MAT DMR PAT allele	PAT DMR MAT allele
H3	H3K4ac	Tail	CMM	Body		81 ± 6	69 ± 11	82 ± 5	
	H3K9ac	Tail	CMM	TSS	Spec>	92 ± 2	82 ± 3	92 ± 2	79 ± 3
	H3K9ac-N*	Tail	CMM	TSS	Spec>	93 ± 2	84 ± 3	93 ± 2	84 ± 2
	H3K18ac	Tail	CMM	TSS		84 ± 4	76 ± 6	84 ± 4	76 ± 6
	H3K27ac	Tail	CMM	TSS	Spec>	79 ± 9	59 ± 15	84 ± 8	
	H3K36ac	Tail	CMM	TSS	Spec>>	78 ± 8	61 ± 8	82 ± 6	
	H3K64ac	Globular			Spec>	81 ± 11	54 ± 12	86 ± 11	
	H3K79ac	Globular			Spec>>	75 ± 5	65 ± 5	76 ± 5	66 ± 5
	Average H3					82 ± 6	69 ± 10	85 ± 6	76 ± 7
H4	H4K5ac	Tail	CMM	Body	Spec>>	77 ± 3	72 ± 4	77 ± 3	72 ± 4
	H4K8ac	Tail	CMM	Body	Spec>	66 ± 2	67 ± 5	66 ± 2	67 ± 5
	H4K12ac	Tail		Body	Spec>>	79 ± 2	74 ± 3	79 ± 2	74 ± 3
	H4K16ac*	Tail		Body	Spec>>	77 ± 3	66 ± 2	77 ± 3	61 ± 2
	H4K91ac*	Globular	CMM	TSS		80 ± 5	69 ± 11	80 ± 4	72 ± 8
	Average H4					76 ± 6	70 ± 3	76 ± 6	69 ± 5
H2A	H2AK5ac	Tail	CMM	Subtelomere		64 ± 2	59 ± 3	64 ± 2	59 ± 3
H2B	H2BK12ac	Tail	CMM	Body		73 ± 3	69 ± 3	73 ± 3	69 ± 3
	H2BK16ac	Tail			Spec>	71 ± 2	66 ± 2	71 ± 2	66 ± 2
	H2BK46ac	Tail			Spec>	73 ± 4	62 ± 6	76 ± 3	63 ± 3
	Average H2B					73 ± 1	66 ± 3	73 ± 2	66 ± 3
	Average					78 ± 8	68 ± 8	79 ± 8	70 ± 7
	Average CMM					79 ± 9	70 ± 8	81 ± 9	73 ± 8
	Average TSS					84 ± 7	72 ± 10	86 ± 5	78 ± 5
	Average body					76 ± 5	69 ± 3	76 ± 5	68 ± 5
	Average spec>>					77 ± 1	68 ± 5	78 ± 2	68 ± 6
	Average spec> or >>					78 ± 8	68 ± 9	80 ± 8	70 ± 8
	Average tail					78 ± 8	69 ± 8	79 ± 9	70 ± 8
	Average globular					79 ± 4	63 ± 8	81 ± 5	69 ± 4

Antibodies are listed in the order of histone types. Asterisk next to the antibody indicates data from Singh *et al.*, 2010 (65). The location of each lysine residue in the histone molecule (tail or globular domain) is indicated. The localization of the individual acetylated lysine residues is classified according to genome-wide mapping data. Acetylated residues typically enriched at the TSS or found at the TSS and also along the gene body (body) (8) or at subtelomers (9) are distinguished. Acetylation sites that belong to the 'common modification module' (CMM) are also marked (8). The specificity of the antibody is indicated when it was tested by our laboratory. Spec>> means that we have high confidence in the antibody, because it only recognizes the acetylated form of its own specific residue. It does not cross-react with any other peptide or with its own unmodified peptide (Supplementary Figure S1). Spec> means that the antibody reacts with its own acetylated peptide and does not cross-react with peptides for other lysine sites. It recognizes or it may weakly recognize its own unacetylated peptide. The percent parental acetylation was calculated for the unmethylated alleles for the maternally and paternally methylated DMRs (paternal allele and maternal allele acetylated, respectively). Average percent acetylation is shown with standard errors obtained from four independent ChIP reactions (two 129 X JF1 and two JF1 X 129 MEF) samples. All data includes each SNuPE measurement from Figures 1–4. Filtered data excludes SNuPE measurements from samples with low level of ChIP. (Samples marked with X in Figures 1–4 and uncolored cells in Supplementary Tables S4 and S5). Average values are calculated for all data and for filtered data. Averages are also calculated for different sub data sets: histone types, localization, location of the lysine in the histone (tail versus globular domain) and confidence in the antibodies.

acetylation bias toward the paternal allele with the control H3K9ac antibody (Figure 1). We obtained similar paternal allele-specific bias with the other 13 histone acetylation antibodies at the maternally methylated DMRs (Figures 1–4).

At the three paternally methylated DMRs, *H19/Igf2* ICR, *Rasgrf1* DMR and IG-DMR H3K9ac was strongly biased toward the maternal allele (65). Now we found that histone acetylation at each lysine residue examined exhibited a maternal-specific bias, with a few exceptions (Figures 1–4). These exceptions usually coincided with very low precipitation levels at that specific DMR with the specific antibody (Supplementary Table S4).

In general, the acetylation bias toward the unmethylated allele was consistent at maternally and paternally methylated DMRs with only a few exceptions. The maternally methylated DMRs exhibited an average of 10% stronger acetylation bias toward the unmethylated allele than the paternally methylated DMRs (78 versus 68%). This was true for each antibody tested except for the H4K8ac antibody (Table 1). This trend did not change (Table 1) when we considered a subset of the data, excluding samples with low precipitation levels (Supplementary Tables S4 and S5), nor when we considered antibodies only with high confidence (Supplementary Figure S1). The greatest acetylation difference between maternally versus paternally methylated DMRs was found at the H3K64 residue (81 versus 54%), but the paternally methylated DMRs had low levels of precipitation with this antibody. The lysine residues in
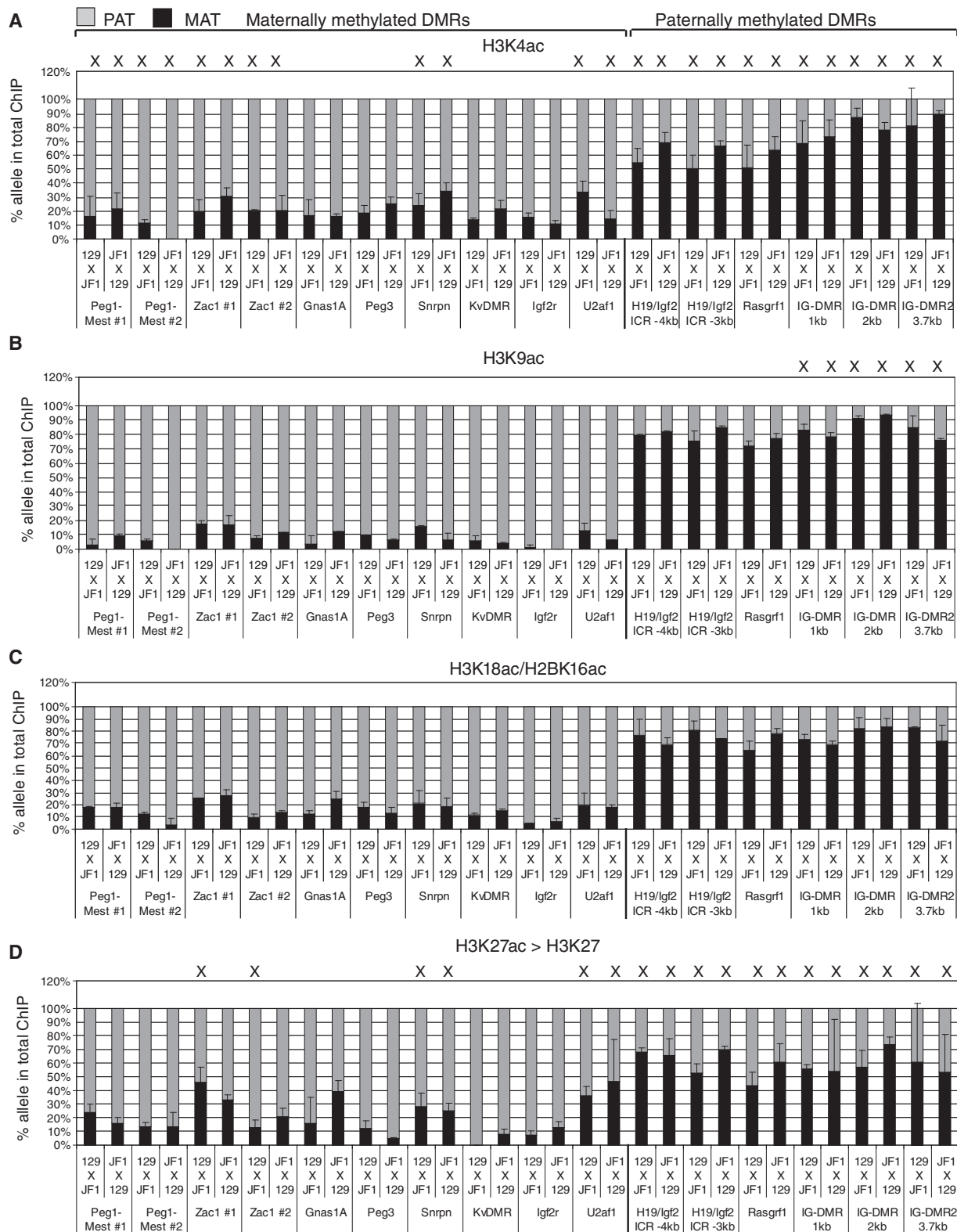
Figure 1. Histone acetylation marks in the tail of H3 distinguish the CpG-unmethylated alleles of maternally and paternally methylated DMRs. Allele specific histone acetylation was determined at SNPs within maternally methylated (Peg1, Zac1, Gnas1A, Peg3, Snrpn, Igf2r, U2af1 DMRs and KvDMR1) and paternally methylated DMRs (H19/Igf2, Rasgrf1 DMRs and IG-DMR) by quantitative 16-plex assays (65). Alternative SNPs were included for the H19/Igf2 ICR (-3 kb and -2 kb from the TSS of H19), IG-DMR (at 1, 2 or 3.7 kb along the DMR), Peg1-Mest (#1 and #2 along the DMR) and Zac1 (#1 and #2) DMRs. ChIP was performed in duplicates using antibodies against specific modified histones (indicated on the top of each row of charts) from 129 mother X JF1 father or the reciprocal JF1 mother X 129 father MEFs (indicated under each column, maternal allele comes first). The ratio of an allele-specific histone modification at a specific region was expressed as a percent of maternal (black bars) or paternal (gray bars) in the total (maternal + paternal, or 100%) of immunoprecipitation. Standard deviations are indicated as error bars. X above the bars indicates low precipitation values with the indicated antibody at the specific DMR (<25 copies measured from 3 out of 100 µl ChIP elution (Supplementary Tables S4 and S5). Data obtained with (**A**) H3K4ac, (**B**) H3K9ac, (**C**) H3K18ac and (**D**) H4K27ac are presented. The maternally methylated DMRs exhibited a paternal allele-specific bias for histone acetylation marks whereas the paternally methylated DMRs were more maternally biased.
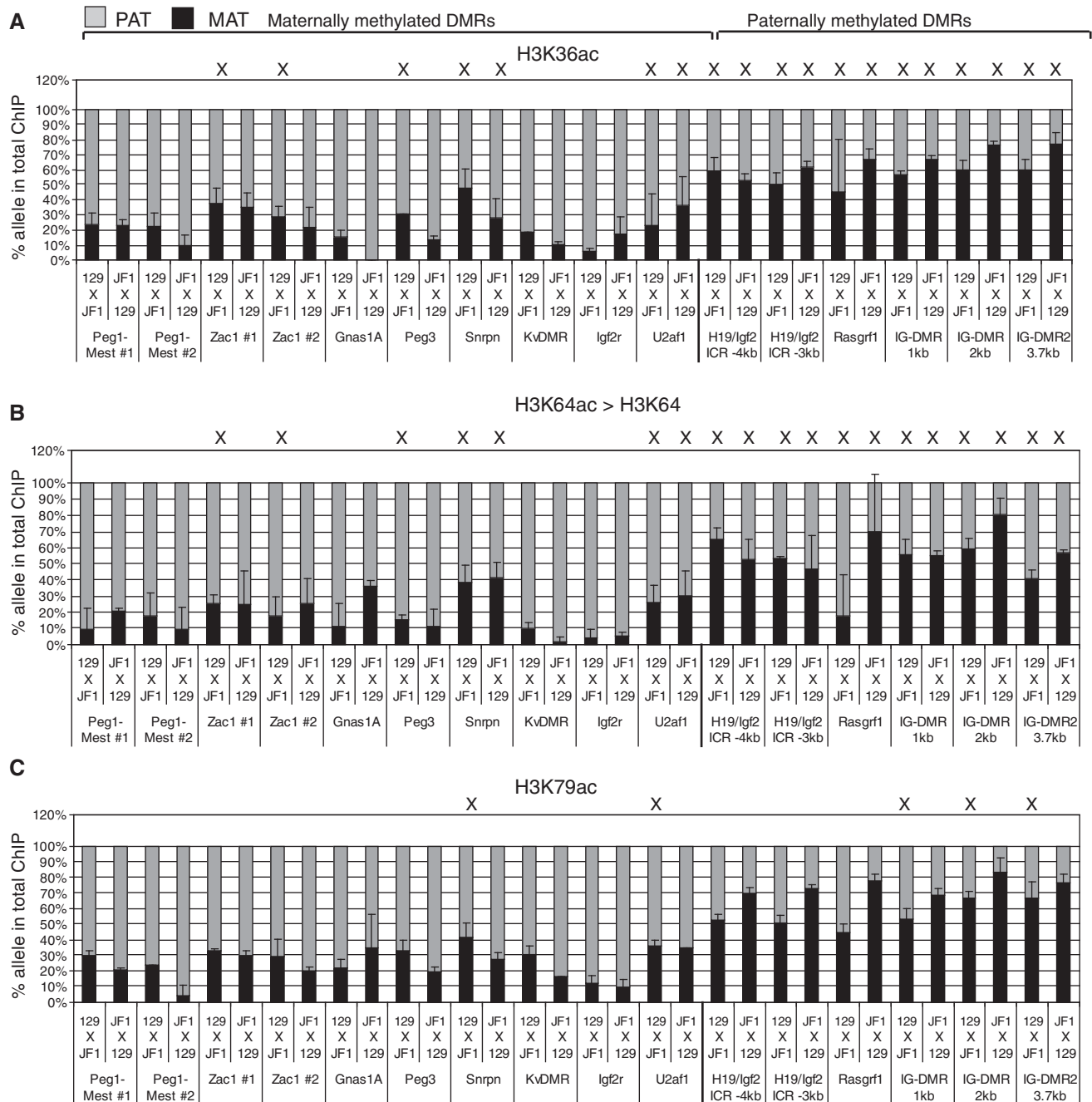
Figure 2. Histone acetylation marks in the tail and globular domain of H3 at DMRs. (**B**) H3K64ac and (**C**) H3K79ac globular domain modifications are comparable to the H3 histone tail mark (**A**) H3K36ac. Other details are as in Figure 1.

the histone globular domains versus tails did not show a difference in allele-specific acetylation bias. The strength of allelic bias at both maternally and paternally methylated DMRs was different depending on the histone type. H3 bias was the strongest, followed by H4, and the other two core histones, H2B and H2A. The allelic bias was strongest with the H3K9ac antibody and weakest with the H2AK5ac antibody. The H3K27ac and H3K64ac antibodies showed only a very low level (59 and 54%, respectively) of bias at the paternally methylated DMRs. We found that the allele-specific acetylation at lysine sites

that belong to the common modification module (8) was only very slightly higher than lysine sites in general. Acetylated lysine residues that are normally enriched at TSSs (8), however, exhibited higher allele-specificity than the average of all acetylation sites examined (Table 1) at both maternally (84 versus 78%) and paternally (72 versus 68%) methylated DMRs.

Allele-specific histone acetylation in embryos

To test the key findings obtained with MEFs, and to demonstrate their widespread relevance, we examined
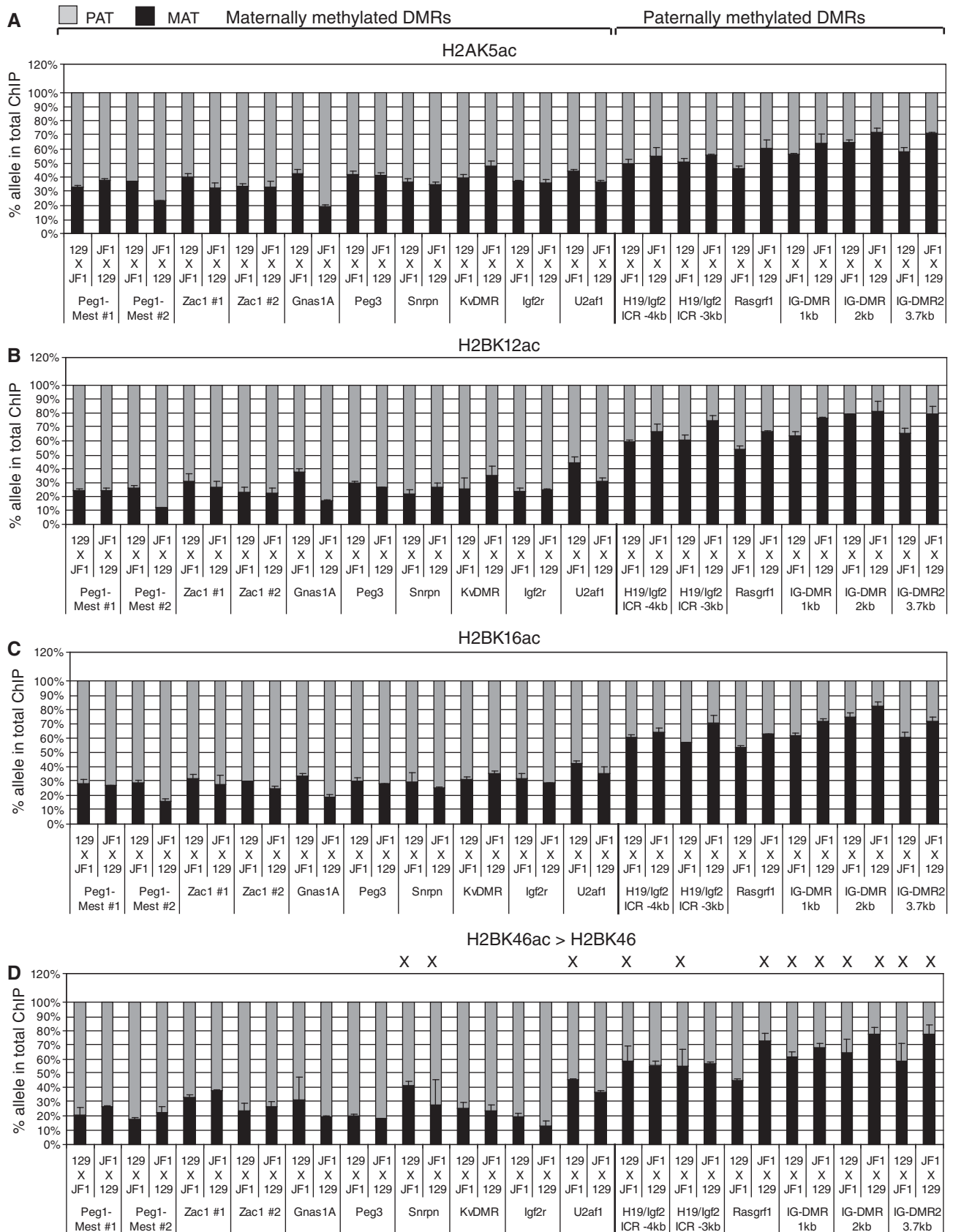
Figure 3. Histone acetylation marks in the tail of H4 at DMRs. (**A**) H4K5ac, (**B**) H4K8ac and (**C**) H4K12ac antibodies were used. Other details are as in Figure 1.

allele-specific histone acetylation at DMRs in the body, head and placenta of 13.5 dpc JF1 X 129 embryos with four histone acetylation antibodies. Acetylation levels at DMRs were higher than at repeat elements and lower than at the *c-myc* promoter, similarly to MEFs (Supplementary Table S6). Acetylation levels were higher in the body and head than in the placenta. Maternally methylated DMRs had higher acetylation levels than paternally methylated DMRs. Each DMR exhibited parental allele-specific histone acetylation at each K residue analyzed (Figure 5). The DNA-hypomethylated allele was more

acetylated, similarly to MEFs. The bias was stronger in the body and head, but weaker in the placenta. The allelic acetylation bias in the body and head was higher at maternally versus paternally methylated DMRs with the H3K9ac antibody (12 and 9%, respectively) (Supplementary Table S7), similarly to MEFs, where the difference was 10% (Table 1). The H4K5ac, H4K12ac and H2BK16ac antibodies revealed smaller differences between maternally and paternally methylated DMRs in MEFs, and this was consistent in the body and head of 13.5 dpc embryos. Placenta chromatin exhibited

Figure 4. Histone acetylation marks in the tail of H2A and H2B at DMRs. (**A**) H2AK5ac, (**B**) H2BK12ac, (**C**) H2BK16ac and (**D**) H2BK46ac antibodies were used.
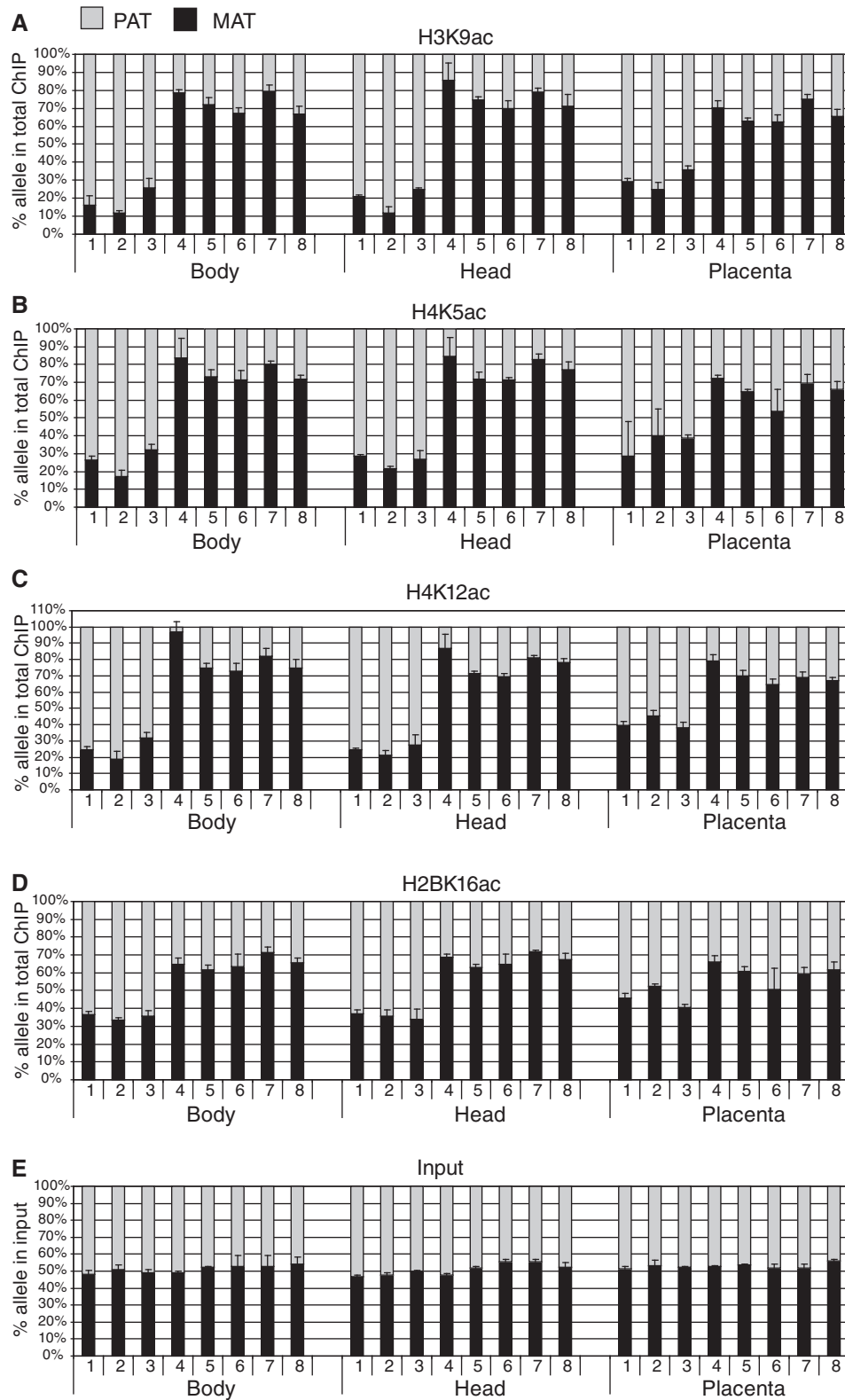
Figure 5. Histone acetylation marks distinguish the CpG-unmethylated alleles of maternally and paternally methylated DMRs in embryos. Allele specific histone acetylation was determined within eleven DMRs by quantitative 16-plex assays (65). Data obtained at the *Zac1* (samples 1 and 2), *Snrpn* (sample 3), *H19/Igf2* (samples 4 and 5*)* and IG-DMR (samples 6–8) DMRs are shown. ChIP was performed in triplicates using the body, head and placenta samples of 13.5 dpc embryos from the cross of JF1 mother X 129 father. Data with (**A**) H3K9ac, (**B**) H4K5ac, (**C**) H4K12ac and (**D**) H2BK16ac antibodies are presented. The maternally and paternally methylated DMRs exhibited paternal and maternal allele-specific bias for histone acetylation, respectively. Body and head exhibited stronger allele-specific acetylation bias than placenta. There was no allele-specific bias in the input chromatin samples (**E**). The maternal cell contamination was undetectable in the placenta. Other details are as in Figure 1.

acetylation bias between alleles, but it was less pronounced and the bias was not different between maternally and paternally methylated DMRs.

Allele-specific chromatin is expected to be associated with allele-specific gene expression. We previously analyzed the allele-specific expression of several imprinted genes in MEFs (36,65) embryos (66). Now we analyzed the body, head and placenta of 13.5 dpc embryos for overall level and allele-specific expression of five imprinted genes, associated with two maternally and two paternally methylated DMRs. We found that the expression of each imprinted gene was strongly biased toward the expected parental allele in the body, head and the placenta of 13.5 dpc embryos regardless of wide differences in normalized expression levels (Supplementary Figure S3). Allele-specific chromatin differences at the maternally methylated *Snrpn*, *Zac1*, and the paternally methylated IG-DMR and *H19*/*Igf2* ICR DMRs were in agreement with known paternal allele-specific expression of *Snrpn*, *Zac1*, *Igf2* and maternal allele-specific expression of *Gtl2* and *H19* imprinted genes. Interestingly, in placenta, the allele-specific expression of imprinted genes was stricter than the allele-specific histone acetylation at these DMRs.

Allele-specific histone acetylation at the *H19*/*Igf2* imprinted region

We investigated the parental allele-specific enrichment of histone covalent modifications at the *H19*/*Igf2* imprinted domain using the 7-plex Sequenom assay and the promoter assay (65). We found that the histone acetylation marks were strongly paternal-allele specific at the *Igf2* DMR1, *Igf2* P2 promoter and the *Igf2* DMR2 sequences (Figures 6–8) similarly to the H3K9ac pattern (36). The *H19*/*Igf2* ICR and the *H19* gene body, however, showed only slight bias toward the maternal allele. This pattern was different from the strongly maternally biased H3K9ac pattern (36) but was similar to the H4K91ac pattern (65). The *H19* promoter was unusual: despite being transcribed in MEFs from the maternal allele (36), it only exhibited maternal allele-specific bias for H3K9ac (36) and H3K18ac but did not exhibit maternal allele-specific bias for the other acetylated lysines characteristic of active or poised promoters (8). The intermediary region at −8 kb exhibited slight paternal allele-specific bias with each of the acetylation antibodies.

Effects of the ICR-CTCF site mutations on the allele-specific histone acetylation at the *H19*/*Igf2* imprinted domain

We have shown earlier that CTCF binding in the *H19*/*Igf2* ICR is essential for organizing the maternal allele's chromatin composition (36,65). With regard to histone tail modifications, CTCF binding in the maternal allele recruited active chromatin at the *H19* locus and repressive chromatin at the *Igf2* locus, and also excluded repressive chromatin at the *H19* locus and active chromatin from the *Igf2* locus (36). CTCF did not recruit globular domain modifications to the maternal allele, rather excluded them from the maternal allele at the *Igf2* locus (65). We asked how general the role of CTCF is in organizing histone acetylation along this imprinted domain. We compared 129 X CS and mutant CTCFm X CS MEF chromatin along the domain (Supplementary Figure S2). The latter cells lacked *in vivo* ICR-CTCF binding (36) due to point mutations at each of the four CTCF binding sites in the ICR (36,61). Disabled insulation resulted in biallelic *Igf2* expression and lack of *H19* expression in CTCFm X CS fetal kidneys and livers (61) and in CTCFm X CS MEFs (36). We measured the amount of immunoprecipitated DNA from equal amounts of chromatin in normal versus mutant cells using real-time PCR (Supplementary Figure S2) and determined the parental allele-specificity of chromatin in the mutant cells using ChIP-SNuPE (Figures 6–8).

Remarkably, histone acetylation at each lysine residue became biallelic in the mutant cells at the *Igf2* DMR1, P2 promoter and DMR2 (Figures 6–8), where it was paternal allele-specific in normal cells, providing evidence that CTCF binding in the ICR is required for excluding acetylation from the maternal allele at the *Igf2* locus at a distance. The change in allele-specificity was accompanied by an increase in precipitation levels at the DMR1, but not at the *Igf2* promoter and DMR2. Histone acetylation at each lysine residue switched from slightly maternal to biallelic at the ICR and *H19* gene body (Figures 6–8) and this was accompanied by a decrease in the level of precipitation (Supplementary Figure S2). These data suggest that CTCF has a slight effect on the recruitment of histone acetylation at the *H19* ICR and gene body. We noticed that H2BK16ac decreased at each region across the domain except at the *Igf2* DMR1.

DISCUSSION

In this study, we provide a map of the allele-specific acetylation of four histones at 13 different lysine residues, H3K4, H3K18, H3K27, H3K36, H3K79, H3K64, H4K5, H4K8, H4K12, H2AK5, H2BK12, H2BK16 and H2BK46 at 11 DMRs in reciprocal mouse crosses in MEFs. We show that histone acetylation in histones H3, H4, H2A and H2B allele-specifically marks the unmethylated alleles of each germ line DMRs. Maternally methylated DMRs, that usually overlap with transcriptional start sites, in general exhibited higher level of acetylation and stronger allele-specific bias than paternally methylated DMR that reside in intergenic regions. Because allele-specific acetylation bias always occurs toward the unmethylated allele, our results argue that a whole group of enzymes with HAT and HDAC activities must be coordinately regulated to maintain allele-specific histone acetylation of the DMRs at a wide range of lysine residues. These activities likely occur as maintenance mechanisms of monoallelic transcription regulation such as promoter and insulator functions. We confirmed monoalleleic expression of imprinted genes and histone acetylation in 13.5 dpc embryos at two maternally methylated DMRs and two paternally methylated
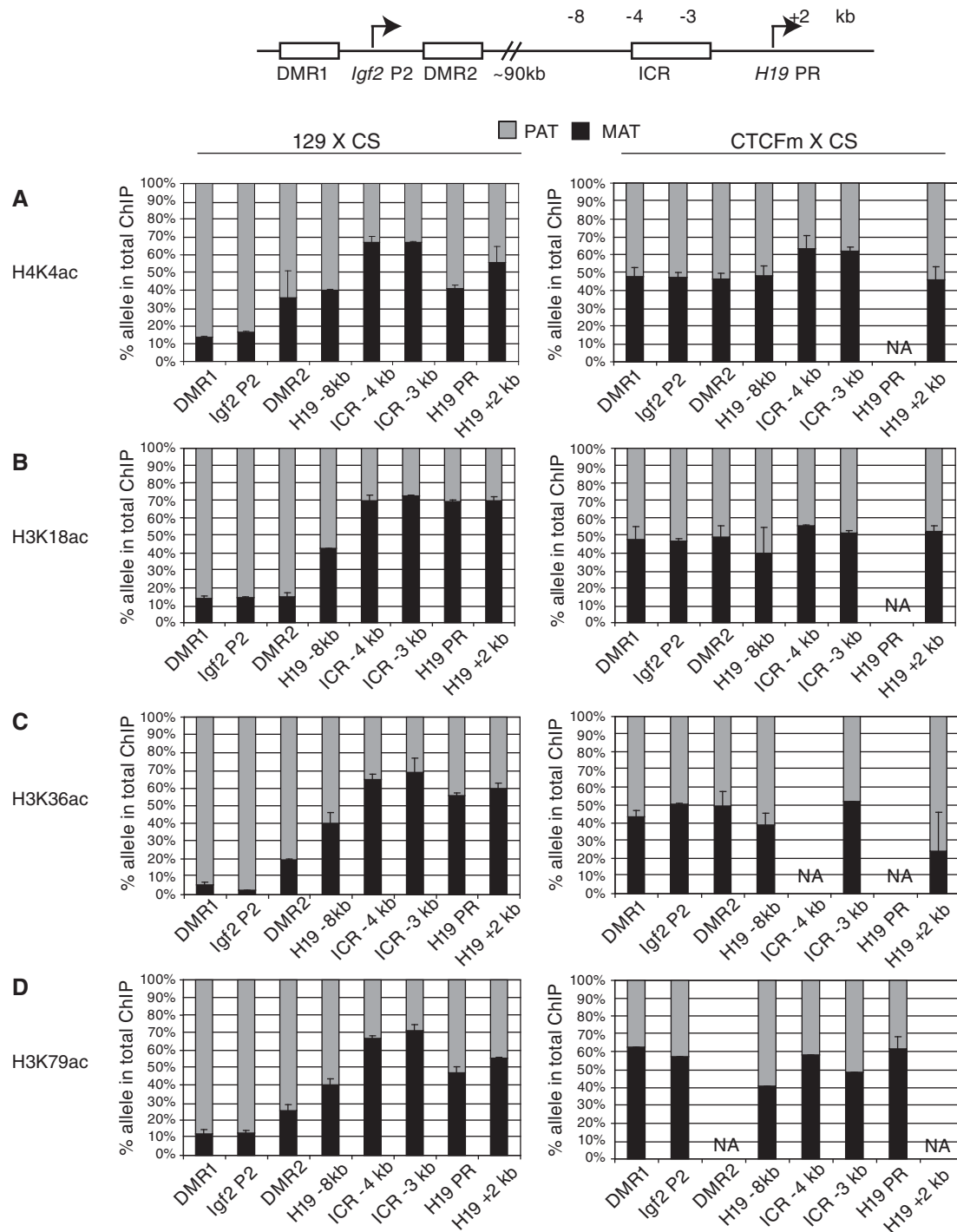
Figure 6. Histone H3 acetylation along the *H19/Igf2* imprinted domain. Allele-specific activating chromatin was measured by quantitative ChIP-SNuPE assays at the *H19/Igf2* imprinted domain, using a 7-plex assays (65) and the *H19* promoter assay. The regions of interest are depicted in the schematic drawing and indicated under each column. ChIP was done in duplicates using antibodies against specific histone modifications (indicated on the left side of each row of charts) to precipitate chromatin from normal 129 X CS (129 mother X CS father) or mutant CTCFm X CS (CTCFm mother X CS father) MEFs (indicated at the top). The precipitated chromatin was not sufficient in some cases to measure the allelic ratio (N/A). (**A**) H3K4ac, (**B**) H3K18ac, (**C**) H3K36ac and (**D**) H3K79ac clearly distinguished the paternal allele at the *Igf2* regions. These modifications were slightly biased or not biased toward the maternal allele at the *H19* ICR and gene body. Weak paternal allele-specific acetylation existed at a 'neutral' intermediary region −8 kb upstream of the *H19* promoter. Allele-specific acetylation bias along the domain was only apparent in normal cells but not in CTCF site mutant cells.
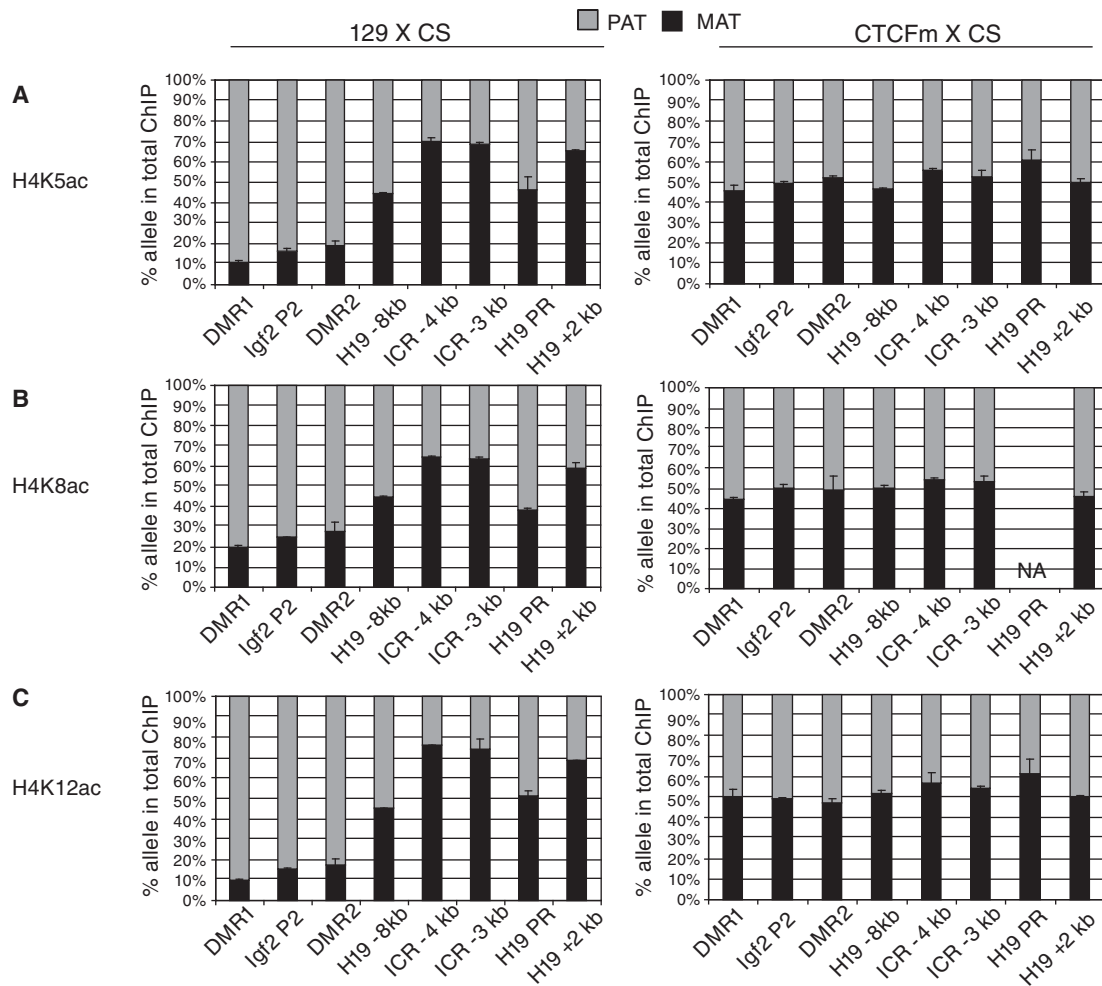
Figure 7. H4 acetylation along the *H19/Igf2* imprinted domain. (**A**) H4K5ac, (**B**) H3K8ac and (**C**) H4K12ac marks. Other details are as in Figure 6.

DMRs. We provide evidence that along the *H19/Igf2* imprinted domain CTCF insulator binding controls allele-specific histone acetylation at each lysine residue.

The allele-specific distribution of histone acetylation is inversely correlated with the methylation of DMRs

To obtain a general assessment of histone acetylation at DMRs of imprinted gene clusters, we mapped the allele-specific acetylation in the core histones at a wide range of lysine residues. We provided quantitative information using ChIP-SNuPE assays on allele-specific histone acetylation at 11 DMRs with antibodies against 13 specific lysine residues. We revealed that acetylation bias distinguishes the parental alleles at each DMR with only few exceptions. The results were consistent with our previous findings regarding H3K9ac, H4K91ac and H4K16ac (65). At the maternally methylated DMRs, a paternal-allele specific bias was evident whereas at the paternally methylated DMRs, a maternal-allele specific bias was evident for histone acetylation. All tested histone acetylation antibodies in the four canonical histones displayed similar trends. Allele-specific acetylation bias at DMRs was confirmed in the body, head and the placenta of 13.5 dpc embryos. These findings altogether

point to the role of histone acetylation as an active chromatin mark in the unmethylated allele of DMRs.

The bias observed at DMRs for the 'common modification module' residues (8) did not differ significantly from the general acetylation difference, but acetylation sites enriched at TSS showed stronger allele-specificity at DMRs. There were differences in the amplitude of the bias between lysine residues, suggesting that different histone residues may respond slightly differently to the commands that determine allele-specific chromatin. The strongest bias was found at H3K9ac (36) whereas the weakest bias was found at H2AK5ac. Interestingly, H2AK5ac is one of the rare acetylated residues found at subtelomeric regions, in the proximity of constitutive heterochromatin (9). Allele-specific acetylation was more relaxed in placenta than in the body or head of the embryo at 13.5 dpc, suggesting that the recruitment and or maintenance of histone acetylation involves tissue-specific components at DMRs.

The allele-specificity of histone acetylation in the four canonical histones suggests that histone acetylation in each core histones at many lysine residues may have functional relevance at DMRs. Acetylated histones in the unmethylated allele may destabilize nucleosomes, leading
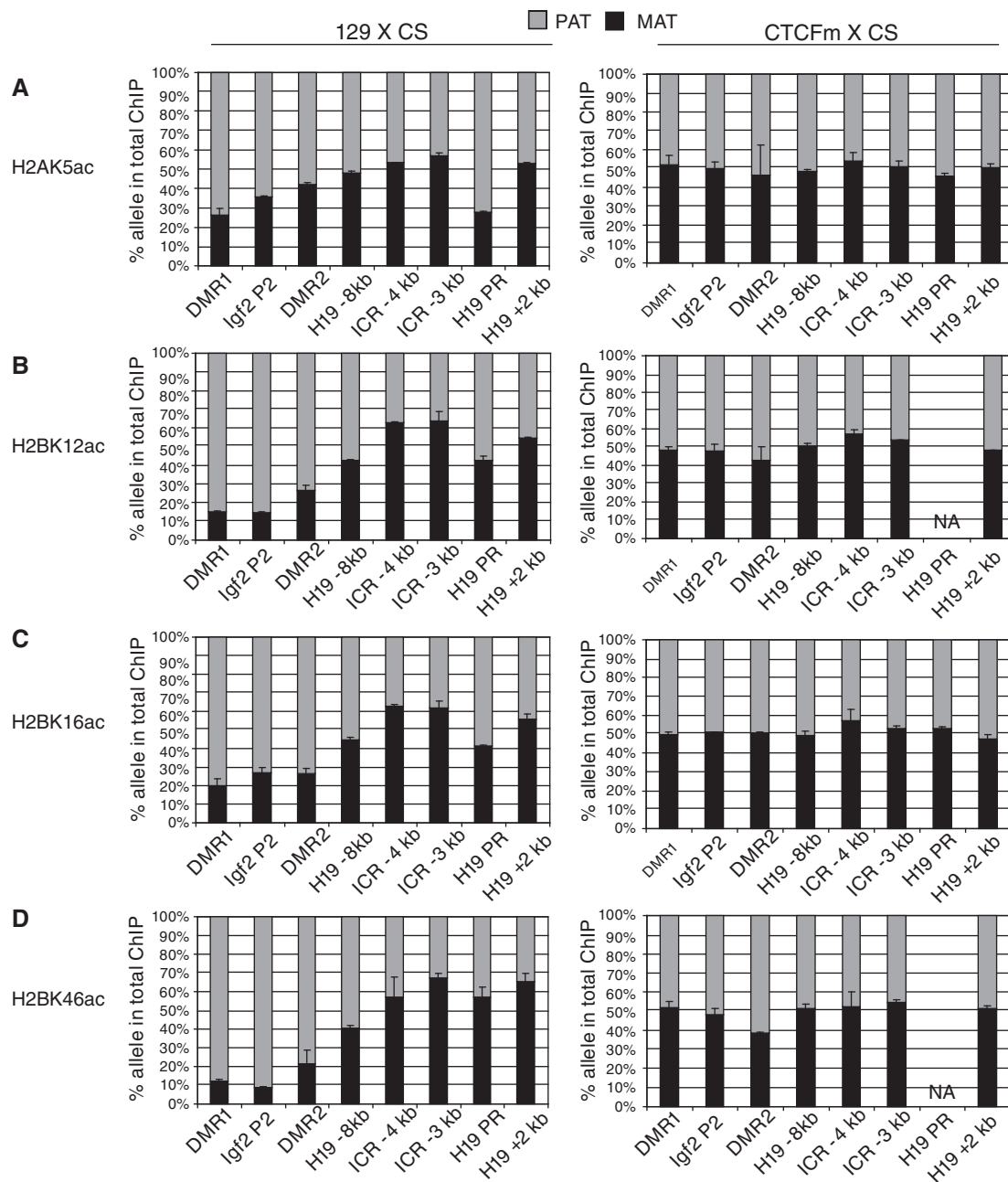
Figure 8. Histone acetylation marks in the tails of H2A and H2B along the *H19/Igf2* imprinted domain. (**A**) H2AK5ac, (**B**) H2BK12ac, (**C**) H2BK16ac and (**D**) H2BK46ac antibodies were used. Other details are as in Figure 6.

to a more accessible chromatin. Core histone acetylation alters the ability of H1 linker histones to condense active chromatin (67). Dynamic acetylation–deacetylation increases the lability of H2A-H2B dimers, and allows remodeling of chromatin and incorporating histone variants into the nucleosome (68,69), therefore, increases the accessibility of the DNA. Strict parental allele-specific histone acetylation along the DMR, however, may not be required for strict monoallelic gene expression. At least in the placenta the allele-specific expression of imprinted genes was stricter than the allele-specific histone acetylation at DMRs. Histone acetylation in the unmethylated parental DMR allele may be more important in providing

chromatin memory of the active allele during cell divisions (70,71).

Allelic acetylation bias is stronger at maternally methylated compared to paternally methylated DMRs

Acetylation patterns associated with promoter activities and/or transcription-through events may be distinct from those belonging to a specific 'histone acetylation imprinting signature' that could constitutively mark unmethylated DMR alleles. Identification of this signature could give important clues on the mechanism involved in maintaining the DNA-hypomethylated state of DMRs. It

may be difficult to discern a pure 'histone acetylation imprinting signature' at DMRs, because these often harbor elements with general gene regulatory functions.

We tested acetylation at eleven DMRs, and this provided the opportunity to compare histone acetylation between maternally methylated DMRs that generally overlap with promoters/transcription units (16), and paternally methylated DMRs that are located in intergenic regions (64). Based on these differences in localization, acetylation is expected to be high at maternally methylated DMRs in the paternal allele where transcription takes place but is not expected to be high in the maternal allele of paternally methylated DMRs in intergenic regions where transcription-associated acetylation is unlikely. Indeed, we did not detect transcription-through events at the *Rasgrf1* DMR, *H19/Igf2* ICR and *IG-DMR* in reverse-transcription PCR using the DMR real-time PCR assays in MEFs and embryo bodies, heads and placentas at 13.5 dpc (Singh,P. and Szabó,P., unpublished data). We found that histone acetylation at both maternally and paternally methylated DMRs marked the hypomethylated allele, but maternally methylated DMRs exhibited higher level of acetylation levels and stronger allelic bias than paternally methylated DMRs. These differences are likely due to the different genomic locations. We showed that *Snrpn* and *Zac1* exhibit strict paternal allele-specific expression at 13.5 dpc. At these DMRs paternal allele-specific histone acetylation may be present because the maternally methylated DMR overlaps with the promoter/transcription unit of the paternally expressed *Snrpn/Snrfn* and the *Zac1* genes, respectively. The presence of maternal allele-specific acetylation in the intergenic paternally methylated *H19/Igf2* DMR, on the other hand, depends on CTCF insulator binding in the maternal allele (Figures 6–8) (36,65). Maternal allele-specific acetylation may also depend on CTCF binding at the other two paternally methylated intergenic DMRs (72,73).

ICRs utilize general regulatory mechanisms of promoters and insulators and perhaps others. ICR DMRs may only be different from regulatory regions of biallelically-expressed genes because germ line events render their regulatory capacity functional in one parental allele and not functional in the other allele and these differences are maintained in the soma. The maintenance of allele-specific chromatin differences in turn depends on the constitutive use of the regulatory functions (promoters and insulators) of the DMRs.

Allele-specific acetylation along the *H19/Igf2* imprinted domain depends on CTCF binding in the ICR

Our present data is consistent with our previous finding that CTCF is the master organizer of chromatin at the *H19/Igf2* imprinted domain (36). Again we found that CTCF was required for specifying the maternal allele's chromatin. CTCF sites in the ICR were required for slight maternal acetylation bias at the *H19* locus and for strong paternal bias at the *Igf2* locus. CTCF may directly or indirectly recruit acetylation marks to the maternal

allele at the ICR and exclude them from the maternal allele at the *Igf2* locus. HATs and HDACs co-localize with histone acetylation in the genome (7) to set the steady-state level of histone acetylation at active and poised alleles. If CTCF has a direct role in setting histone acetylation marks in the maternal allele, it may do so by recruiting HATs and HDACs at the ICR.

CTCF controls DNA methylation at the ICR and distantly at the *Igf2* DMRs (36,61–63). Because the *H19* promoter is unmethylated in CTCFm X CS MEFs (36) attaining biallelic histone acetylation in these cells is not a consequence of methylation change at the promoter. CTCF was shown to control histone tail modifications at the *H19* promoter indirectly by setting the activity state of the promoter (49). It is likely that in the CTCF site mutant MEFs the maternal allele-specific acetylation is lost due to loss of CTCF-mediated initiation of *H19* transcription in the embryo and the residual acetylation is biallelic.

HATs and HDACs must act in concert at DMRs

Our results at 11 DMRs and also along the *H19/Igf2* domain argue that a whole group of enzymes with HAT and HDAC activities must be coordinately regulated to establish/maintain allele-specific histone acetylation of DMRs of imprinted genes at a wide range of lysine residues. HATs and HDACs co-localize with histone acetylation at active or poised gene promoters and enhancers in the genome (7) and are expected to co-localize with histone acetylation at the unmethylated allele of DMRs. Lack of general histone acetylation and the predicted absence of HDAC enzymes in the methylated DMR alleles is consistent with the findings that in normal MEFs HDAC inhibitors failed to reactivate the silent alleles of a set of imprinted genes, *H19*, *Igf2r* and *Snrpn* and only slightly reactivated *Igf2* (44,74). In another set of experiments only 2 out of 12 imprinted genes, *Igf2* and *p57(Kip2)* or *Cdkn1c*, became reactivated after trichostatin A treatment in uniparental MEFs (75), but no *Igf2* reactivation was found after Na-butyrate treatment in MatDup.dist7 cells (76). No change in allele-specific acetylation was observed at the *U2af1-rs1* and *Snrpn* imprinted genes after TSA-induced global acetylation changes in MEFs (34). In the light of genome-wide mapping of HATs and HDACs (7), perturbations in these enzymes are expected to cause change in the acetylated and unmethylated parental allele of DMRs.

It will be interesting to find out whether coordinated regulation of many enzymes involves synchronized action of many different enzymes or a cascade mechanism. It will be interesting to reveal a hierarchy amongst the acetylated forms of different histone lysine residues and also between different covalent modifications. H3K4 methylation facilitates H4K16 and H3K9 acetylation (7,77). Our data are consistent with the possibility that the asymmetry of histone acetylation allelic enrichment is a response to H3K4 methylation in the CpG-hypomethylated allele.

REFERENCES

1. Allfrey,V.G., Faulkner,R. and Mirsky,A.E. (1964) Acetylation and methylation of histones and their possible role in the regulation of RNA synthesis. *Proc. Natl Acad. Sci. USA*, **51**, 786–794.
2. Pogo,B.G., Allfrey,V.G. and Mirsky,A.E. (1966) RNA synthesis and histone acetylation during the course of gene activation in lymphocytes. *Proc Natl Acad SciUSA*, **55**, 805–812.
3. Hebbes,T.R., Clayton,A.L., Thorne,A.W. and Crane-Robinson,C. (1994) Core histone hyperacetylation co-maps with generalized DNase I sensitivity in the chicken beta-globin chromosomal domain. *EMBO J.*, **13**, 1823–1830.
4. Hebbes,T.R., Thorne,A.W. and Crane-Robinson,C. (1988) A direct link between core histone acetylation and transcriptionally active chromatin. *EMBO J.*, **7**, 1395–1402.
5. Chan,S., Attisano,L. and Lewis,P.N. (1988) Histone H3 thiol reactivity and acetyltransferases in chicken erythrocyte nuclei. *J. Biol. Chem.*, **263**, 15643–15651.
6. Hendzel,M.J., Delcuve,G.P. and Davie,J.R. (1991) Histone deacetylase is a component of the internal nuclear matrix. *J. Biol. Chem.*, **266**, 21936–21942.
7. Wang,Z., Zang,C., Cui,K., Schones,D.E., Barski,A., Peng,W. and Zhao,K. (2009) Genome-wide mapping of HATs and HDACs reveals distinct functions in active and inactive genes. *Cell*, **138**, 1019–1031.
8. Wang,Z., Zang,C., Rosenfeld,J.A., Schones,D.E., Barski,A., Cuddapah,S., Cui,K., Roh,T.Y., Peng,W., Zhang,M.Q. *et al.* (2008) Combinatorial patterns of histone acetylations and methylations in the human genome. *Nat. Genet.*, **40**, 897–903.
9. Rosenfeld,J.A., Wang,Z., Schones,D.E., Zhao,K., DeSalle,R. and Zhang,M.Q. (2009) Determination of enriched histone modifications in non-genic portions of the human genome. *BMC Genomics*, **10**, 143.
10. Chicoine,L.G., Schulman,I.G., Richman,R., Cook,R.G. and Allis,C.D. (1986) Nonrandom utilization of acetylation sites in histones isolated from Tetrahymena. Evidence for functionally distinct H4 acetylation sites. *J. Biol. Chem.*, **261**, 1071–1076.
11. Sobel,R.E., Cook,R.G. and Allis,C.D. (1994) Non-random acetylation of histone H4 by a cytoplasmic histone acetyltransferase as determined by novel methodology. *J. Biol. Chem.*, **269**, 18576–18582.
12. Couppez,M., Martin-Ponthieu,A. and Sautiere,P. (1987) Histone H4 from cuttlefish testis is sequentially acetylated. Comparison with acetylation of calf thymus histone H4. *J. Biol. Chem.*, **262**, 2854–2860.
13. Ma,X.J., Wu,J., Altheim,B.A., Schultz,M.C. and Grunstein,M. (1998) Deposition-related sites K5/K12 in histone H4 are not required for nucleosome deposition in yeast. *Proc. Natl Acad. Sci. USA*, **95**, 6693–6698.
14. Megee,P.C., Morgan,B.A., Mittman,B.A. and Smith,M.M. (1990) Genetic analysis of histone H4: essential role of lysines subject to reversible acetylation. *Science*, **247**, 841–845.
15. Ye,J., Ai,X., Eugeni,E.E., Zhang,L., Carpenter,L.R., Jelinek,M.A., Freitas,M.A. and Parthun,M.R. (2005) Histone H4 lysine 91 acetylation a core domain modification associated with chromatin assembly. *Mol. Cell*, **18**, 123–130.
16. Kobayashi,H., Suda,C., Abe,T., Kohara,Y., Ikemura,T. and Sasaki,H. (2006) Bisulfite sequencing and dinucleotide content analysis of 15 imprinted mouse differentially methylated regions (DMRs): paternally methylated DMRs contain less CpGs than maternally methylated DMRs. *Cytogenet. Genome Res.*, **113**, 130–137.
17. Thorvaldsen,J.L. and Bartolomei,M.S. (2007) SnapShot: imprinted gene clusters. *Cell*, **130**, 958.
18. Bourc'his,D., Xu,G.L., Lin,C.S., Bollman,B. and Bestor,T.H. (2001) Dnmt3L and the establishment of maternal genomic imprints. *Science*, **294**, 2536–2539.
19. Kaneda,M., Okano,M., Hata,K., Sado,T., Tsujimoto,N., Li,E. and Sasaki,H. (2004) Essential role for de novo DNA methyltransferase Dnmt3a in paternal and maternal imprinting. *Nature*, **429**, 900–903.
20. Okano,M., Bell,D.W., Haber,D.A. and Li,E. (1999) DNA methyltransferases Dnmt3a and Dnmt3b are essential for de novo methylation and mammalian development. *Cell*, **99**, 247–257.
21. Li,E., Beard,C. and Jaenisch,R. (1993) Role for DNA methylation in genomic imprinting. *Nature*, **366**, 362–365.
22. Bielinska,B., Blaydes,S.M., Buiting,K., Yang,T., Krajewska-Walasek,M., Horsthemke,B. and Brannan,C.I. (2000) De novo deletions of SNRPN exon 1 in early human and mouse embryos result in a paternal to maternal imprint switch. *Nat. Genet.*, **25**, 74–78.
23. Fitzpatrick,G.V., Soloway,P.D. and Higgins,M.J. (2002) Regional loss of imprinting and growth deficiency in mice with a targeted deletion of KvDMR1. *Nat. Genet.*, **32**, 426–431.
24. Lin,S.P., Youngson,N., Takada,S., Seitz,H., Reik,W., Paulsen,M., Cavaille,J. and Ferguson-Smith,A.C. (2003) Asymmetric regulation of imprinting on the maternal and paternal chromosomes at the Dlk1-Gtl2 imprinted cluster on mouse chromosome 12. *Nat. Genet.*, **35**, 97–102.
25. Thorvaldsen,J.L., Duran,K.L. and Bartolomei,M.S. (1998) Deletion of the H19 differentially methylated domain results in loss of imprinted expression of H19 and Igf2. *Genes Dev.*, **12**, 3693–3702.
26. Williamson,C.M., Ball,S.T., Nottingham,W.T., Skinner,J.A., Plagge,A., Turner,M.D., Powles,N., Hough,T., Papworth,D., Fraser,W.D. *et al.* (2004) A cis-acting control region is required exclusively for the tissue-specific imprinting of Gnas. *Nat. Genet.*, **36**, 894–899.
27. Williamson,C.M., Turner,M.D., Ball,S.T., Nottingham,W.T., Glenister,P., Fray,M., Tymowska-Lalanne,Z., Plagge,A., Powles-Glover,N., Kelsey,G. *et al.* (2006) Identification of an imprinting control region affecting the expression of all transcripts in the Gnas cluster. *Nat. Genet.*, **38**, 350–355.
28. Wutz,A., Smrzka,O.W., Schweifer,N., Schellander,K., Wagner,E.F. and Barlow,D.P. (1997) Imprinted expression of the Igf2r gene depends on an intronic CpG island. *Nature*, **389**, 745–749.
29. Yoon,B.J., Herman,H., Sikora,A., Smith,L.T., Plass,C. and Soloway,P.D. (2002) Regulation of DNA methylation of Rasgrf1. *Nat. Genet.*, **30**, 92–96.
30. Carr,M.S., Yevtodiyenko,A., Schmidt,C.L. and Schmidt,J.V. (2007) Allele-specific histone modifications regulate expression of the Dlk1-Gtl2 imprinted domain. *Genomics*, **89**, 280–290.
31. Delaval,K., Govin,J., Cerqueira,F., Rousseaux,S., Khochbin,S. and Feil,R. (2007) Differential histone modifications mark mouse imprinting control regions during spermatogenesis. *EMBO J.*, **26**, 720–729.
32. Fournier,C., Goto,Y., Ballestar,E., Delaval,K., Hever,A.M., Esteller,M. and Feil,R. (2002) Allele-specific histone lysine methylation marks regulatory regions at imprinted mouse genes. *EMBO J.*, **21**, 6560–6570.
33. Grandjean,V., O'Neill,L., Sado,T., Turner,B. and Ferguson-Smith,A. (2001) Relationship between DNA methylation, histone H4 acetylation and gene expression in the mouse imprinted Igf2-H19 domain. *FEBS Lett.*, **488**, 165–169.

34. Gregory,R.I., O'Neill,L.P., Randall,T.E., Fournier,C., Khosla,S., Turner,B.M. and Feil,R. (2002) Inhibition of histone deacetylases alters allelic chromatin conformation at the imprinted U2af1-rs1 locus in mouse embryonic stem cells. *J. Biol. Chem.*, **277**, 11728–11734.

35. Gregory,R.I., Randall,T.E., Johnson,C.A., Khosla,S., Hatada,I., O'Neill,L.P., Turner,B.M. and Feil,R. (2001) DNA methylation is linked to deacetylation of histone H3, but not H4, on the imprinted genes Snrpn and U2af1-rs1. *Mol. Cell. Biol.*, **21**, 5426–5436.

36. Han,L., Lee,D.H. and Szabó,P.E. (2008) CTCF is the master organizer of domain-wide allele-specific chromatin at the H19/Igf2 imprinted region. *Mol. Cell. Biol.*, **28**, 1124–1135.

37. Henckel,A., Nakabayashi,K., Sanz,L.A., Feil,R., Hata,K. and Arnaud,P. (2009) Histone methylation is mechanistically linked to DNA methylation at imprinting control regions in mammals. *Hum. Mol. Genet.*, **18**, 3375–3383.

38. Hu,J.F., Pham,J., Dey,I., Li,T., Vu,T.H. and Hoffman,A.R. (2000) Allele-specific histone acetylation accompanies genomic imprinting of the insulin-like growth factor II receptor gene. *Endocrinology*, **141**, 4428–4435.

39. Lewis,A., Green,K., Dawson,C., Redrup,L., Huynh,K.D., Lee,J.T., Hemberger,M. and Reik,W. (2006) Epigenetic dynamics of the Kcnq1 imprinted domain in the early embryo. *Development*, **133**, 4203–4210.

40. Lewis,A., Mitsuya,K., Umlauf,D., Smith,P., Dean,W., Walter,J., Higgins,M., Feil,R. and Reik,W. (2004) Imprinting on distal chromosome 7 in the placenta involves repressive histone methylation independent of DNA methylation. *Nat. Genet.*, **36**, 1291–1295.

41. Li,T., Vu,T.H., Ulaner,G.A., Yang,Y., Hu,J.F. and Hoffman,A.R. (2004) Activating and silencing histone modifications form independent allelic switch regions in the imprinted Gnas gene. *Hum. Mol. Genet.*, **13**, 741–750.

42. Monk,D., Wagschal,A., Arnaud,P., Muller,P.S., Parker-Katiraee,L., Bourc'his,D., Scherer,S.W., Feil,R., Stanier,P. and Moore,G.E. (2008) Comparative analysis of human chromosome 7q21 and mouse proximal chromosome 6 reveals a placental-specific imprinted gene, TFPI2/Tfpi2, which requires EHMT2 and EED for allelic-silencing. *Genome Res.*, **18**, 1270–1281.

43. Pannetier,M., Julien,E., Schotta,G., Tardat,M., Sardet,C., Jenuwein,T. and Feil,R. (2008) PR-SET7 and SUV4-20H regulate H4 lysine-20 methylation at imprinting control regions in the mouse. *EMBO Rep.*, **9**, 998–1005.

44. Pedone,P.V., Pikaart,M.J., Cerrato,F., Vernucci,M., Ungaro,P., Bruni,C.B. and Riccio,A. (1999) Role of histone acetylation and DNA methylation in the maintenance of the imprinted expression of the H19 and Igf2 genes. *FEBS Lett.*, **458**, 45–50.

45. Regha,K., Sloane,M.A., Huang,R., Pauler,F.M., Warczok,K.E., Melikant,B., Radolf,M., Martens,J.H., Schotta,G., Jenuwein,T. *et al.* (2007) Active and repressive chromatin are interspersed without spreading in an imprinted gene cluster in the mammalian genome. *Mol. Cell*, **27**, 353–366.

46. Sakamoto,A., Liu,J., Greene,A., Chen,M. and Weinstein,L.S. (2004) Tissue-specific imprinting of the G protein Gsalpha is associated with tissue-specific differences in histone methylation. *Hum. Mol. Genet.*, **13**, 819–828.

47. Sanz,L.A., Chamberlain,S., Sabourin,J.C., Henckel,A., Magnuson,T., Hugnot,J.P., Feil,R. and Arnaud,P. (2008) A mono-allelic bivalent chromatin domain controls tissue-specific imprinting at Grb10. *EMBO J.*, **27**, 2523–2532.

48. Umlauf,D., Goto,Y., Cao,R., Cerqueira,F., Wagschal,A., Zhang,Y. and Feil,R. (2004) Imprinting along the Kcnq1 domain on mouse chromosome 7 involves repressive histone methylation and recruitment of Polycomb group complexes. *Nat. Genet.*, **36**, 1296–1300.

49. Verona,R.I., Thorvaldsen,J.L., Reese,K.J. and Bartolomei,M.S. (2008) The transcriptional status but not the imprinting control region determines allele-specific histone modifications at the imprinted H19 locus. *Mol. Cell. Biol.*, **28**, 71–82.

50. Yamasaki-Ishizaki,Y., Kayashima,T., Mapendano,C.K., Soejima,H., Ohta,T., Masuzaki,H., Kinoshita,A., Urano,T., Yoshiura,K., Matsumoto,N. *et al.* (2007) Role of DNA methylation and histone H3 lysine 27 methylation in tissue-specific imprinting of mouse Grb10. *Mol. Cell. Biol.*, **27**, 732–742.

51. Yang,Y., Hu,J.F., Ulaner,G.A., Li,T., Yao,X., Vu,T.H. and Hoffman,A.R. (2003) Epigenetic regulation of Igf2/H19 imprinting at CTCF insulator binding sites. *J. Cell Biochem.*, **90**, 1038–1055.

52. Yang,Y., Li,T., Vu,T.H., Ulaner,G.A., Hu,J.F. and Hoffman,A.R. (2003) The histone code regulating expression of the imprinted mouse Igf2r gene. *Endocrinology*, **144**, 5658–5670.

53. Yoshioka,H., Shirayoshi,Y. and Oshimura,M. (2001) A novel in vitro system for analyzing parental allele-specific histone acetylation in genomic imprinting. *J. Hum. Genet.*, **46**, 626–632.

54. Tremblay,K.D., Duran,K.L. and Bartolomei,M.S. (1997) A 5′ 2-kilobase-pair region of the imprinted mouse H19 gene exhibits exclusive paternal methylation throughout development. *Mol. Cell. Biol.*, **17**, 4322–4329.

55. Tremblay,K.D., Saam,J.R., Ingram,R.S., Tilghman,S.M. and Bartolomei,M.S. (1995) A paternal-specific methylation imprint marks the alleles of the mouse H19 gene. *Nat. Genet.*, **9**, 407–413.

56. Bell,A.C. and Felsenfeld,G. (2000) Methylation of a CTCF-dependent boundary controls imprinted expression of the Igf2 gene. *Nature*, **405**, 482–485.

57. Hark,A.T., Schoenherr,C.J., Katz,D.J., Ingram,R.S., Levorse,J.M. and Tilghman,S.M. (2000) CTCF mediates methylation-sensitive enhancer-blocking activity at the H19/Igf2 locus. *Nature*, **405**, 486–489.

58. Kaffer,C.R., Srivastava,M., Park,K.Y., Ives,E., Hsieh,S., Batlle,J., Grinberg,A., Huang,S.P. and Pfeifer,K. (2000) A transcriptional insulator at the imprinted H19/Igf2 locus. *Genes Dev.*, **14**, 1908–1919.

59. Kanduri,C., Pant,V., Loukinov,D., Pugacheva,E., Qi,C.F., Wolffe,A., Ohlsson,R. and Lobanenkov,V.V. (2000) Functional association of CTCF with the insulator upstream of the H19 gene is parent of origin-specific and methylation-sensitive. *Curr. Biol.*, **10**, 853–856.

60. Szabo,P., Tang,S.H., Rentsendorj,A., Pfeifer,G.P. and Mann,J.R. (2000) Maternal-specific footprints at putative CTCF sites in the H19 imprinting control region give evidence for insulator function. *Curr. Biol.*, **10**, 607–610.

61. Szabó,P.E., Tang,S.H., Silva,F.J., Tsark,W.M. and Mann,J.R. (2004) Role of CTCF binding sites in the Igf2/H19 imprinting control region. *Mol. Cell. Biol.*, **24**, 4791–4800.

62. Schoenherr,C.J., Levorse,J.M. and Tilghman,S.M. (2003) CTCF maintains differential methylation at the Igf2/H19 locus. *Nat. Genet.*, **33**, 66–69.

63. Pant,V., Mariano,P., Kanduri,C., Mattsson,A., Lobanenkov,V., Heuchel,R. and Ohlsson,R. (2003) The nucleotides responsible for the direct physical contact between the chromatin insulator protein CTCF and the H19 imprinting control region manifest parent of origin-specific long-distance insulation and methylation-free domains. *Genes Dev.*, **17**, 586–590.

64. Chotalia,M., Smallwood,S.A., Ruf,N., Dawson,C., Lucifero,D., Frontera,M., James,K., Dean,W. and Kelsey,G. (2009) Transcription is required for establishment of germline methylation marks at imprinted genes. *Genes Dev.*, **23**, 105–117.

65. Singh,P., Han,L., Rivas,G.E., Lee,D.H., Nicholson,T.B., Larson,G.P., Chen,T. and Szabó,P.E. (2010) Allele-specific H3K79 Di-versus trimethylation distinguishes ppposite parental alleles at imprinted regions. *Mol. Cell. Biol.*, **30**, 2693–2707.

66. Szabó,P.E. and Mann,J.R. (1995) Allele-specific expression and total expression levels of imprinted genes during early mouse development: implications for imprinting mechanisms. *Genes Dev.*, **9**, 3097–3108.

67. Ridsdale,J.A., Hendzel,M.J., Delcuve,G.P. and Davie,J.R. (1990) Histone acetylation alters the capacity of the H1 histones to condense transcriptionally active/competent chromatin. *J. Biol. Chem.*, **265**, 5150–5156.

68. Li,W., Nagaraja,S., Delcuve,G.P., Hendzel,M.J. and Davie,J.R. (1993) Effects of histone acetylation, ubiquitination and variants on nucleosome stability. *Biochem. J.*, **296 (Pt 3)**, 737–744.

69. Perry,C.A., Dadd,C.A., Allis,C.D. and Annunziato,A.T. (1993) Analysis of nucleosome assembly and histone exchange using

antibodies specific for acetylated H4. *Biochemistry*, **32**, 13605–13614.

70. Jeppesen,P. (1997) Histone acetylation: a possible mechanism for the inheritance of cell memory at mitosis. *Bioessays*, **19**, 67–74.

71. Wade,P.A., Pruss,D. and Wolffe,A.P. (1997) Histone acetylation: chromatin in action. *Trends Biochem. Sci.*, **22**, 128–132.

72. Yoon,B., Herman,H., Hu,B., Park,Y.J., Lindroth,A., Bell,A., West,A.G., Chang,Y., Stablewski,A., Piel,J.C. *et al.* (2005) Rasgrf1 imprinting is regulated by a CTCF-dependent methylation-sensitive enhancer blocker. *Mol. Cell. Biol.*, **25**, 11184–11190.

73. Takada,S., Paulsen,M., Tevendale,M., Tsai,C.E., Kelsey,G., Cattanach,B.M. and Ferguson-Smith,A.C. (2002) Epigenetic analysis of the Dlk1-Gtl2 imprinted domain on mouse chromosome 12: implications for imprinting control from comparison with Igf2-H19. *Hum. Mol. Genet.*, **11**, 77–86.

74. Mann,J.R. and Szabó,P.E. (2004) Genomic imprinting in mouse embryonic stem and germ cells. In Sell,S. (ed.), *Stem Cell Handbook*. Humana Press, Totowa, NJ, pp. 81–88.

75. El Kharroubi,A., Piras,G. and Stewart,C.L. (2001) DNA demethylation reactivates a subset of imprinted genes in uniparental mouse embryonic fibroblasts. *J. Biol. Chem.*, **276**, 8674–8680.

76. Eversole-Cire,P., Ferguson-Smith,A.C., Sasaki,H., Brown,K.D., Cattanach,B.M., Gonzales,F.A., Surani,M.A. and Jones,P.A. (1993) Activation of an imprinted Igf 2 gene in mouse somatic cell cultures. *Mol. Cell. Biol.*, **13**, 4928–4938.

77. Pray-Grant,M.G., Daniel,J.A., Schieltz,D., Yates,J.R. III and Grant,P.A. (2005) Chd1 chromodomain links histone H3 methylation with SAGA- and SLIK-dependent acetylation. *Nature*, **433**, 434–438.